

Z. Soltanzadeh,
S. Shaikhzadeh Najar*,
M. Haghpanahi¹,
M. R. Mohajeri-Tehrani²

Prediction of Compression Properties of Single Jersey Weft-knitted Fabric by Finite Element Analysis Based on the Hyperfoam Material Model

DOI: 10.5604/12303666.1191431

Department of Textile Engineering,
Amirkabir University of Technology,

¹Department of Mechanics,
Iran University of Science and Technology,

²Endocrinology and Metabolism Research Center,
Tehran University of Medical Sciences,

Tehran, Iran

*Corresponding author: e-mail: saeed@aut.ac.ir

Abstract

A 3-D finite element model based on the hyperfoam material model was developed in order to predict the compression behaviour of knitted fabrics in a large deformation state. The degree of compressibility of the fabric is determined by the extent of its volume reduction under external pressure. The compression properties of nine produced knitted fabrics at eight pressure values (2.04, 5.10, 10.19, 20.39, 50.97, 101.94, 152.90, and 203.87 kPa) were measured using a fabric thickness tester and results were compared with finite element results. The FEM results of fabric thickness changes (ΔT) and fabric compressibility (EMC) showed good agreement with experimental results, with an average error of 5 and 4.9 percent, respectively. However, the results of fabric linearity of the compression (LC) and work of compression (WC) showed fair agreement, with an average error of 24.5 and 24 percent, respectively.

Key words: fabric compression, three-dimensional FEM, mechanical properties, weft-knitted fabrics, contact mechanics.

Introduction

One of the most important mechanical properties of fabric along with bending, tensile and shear is fabric compression. A fabric that compresses easily is likely to be judged as soft, possessing a low modulus or highly compressible. Compression is also fundamentally important in determining how a fabric will perform when subjected to a wide range of complex deformations. In surgical compression, the softness of fabric is important for two main reasons: The fabric should give rise to minimal skin irritation during prolonged wear and, while maximising the chances for the patient, comply with the extended plastic surgery recovery period [1].

The lateral compressive behaviour of fibre assemblies was first investigated by Van Wyk [2]. Later on, de-Jong *et al.* [3] modified Van Wyk's model and proposed the two parameters equation to predict the compression behaviour of wool woven fabrics. Norman B. Bell and William W. Roberts [4] presented a model that allows prediction of the properties of a fibre assembly under compression from the physical properties of its component fibres, taking into account both static and kinetic friction. The authors used computer simulation and compared their results with van Wyk's Theory. Gurumurthy [5] and Murthyguru [6] predicted the compression characteristics of fabrics by using neural networks. To analyse the compression behaviour of

knitted structures, Bakhtiari *et al.* [7] used the two parameters model proposed by de-Jong *et al.* [3]. Xu-hong and Ming-qiao [8] introduced a primary mechanical model to describe the compressive deformation of spacer fabric. Lin *et al.* [9] investigated the mechanical behaviour of woven fabric under compression using 3D finite element analysis in conjunction with a nonlinear mechanical model for the yarn. Vassiliadis *et al.* [10] predicted the compressional behaviour of warp-knitted spacer fabrics by two-scale (micro and macro) mechanical analysis using FEM. Sheikhzade *et al.* [11] adapted Van Wyk's equation and predicted the lateral compressive behaviour of spacer fabrics. Gunasekaran *et al.* [1] attempted to formulate a new single parameter of compression using the least squared method. Computation of the new measurement is done by means of an analysis of the Kawabata pressure-thickness curve.

It may be considered that there have been some attempts to predict the compression behaviour of woven fabric [3, 5, 9], the knitted structure [1, 7] and spacer fabric [8, 10, 11].

However, to our knowledge there is no published work predicting the compression properties of single jersey weft knitted fabrics using the finite element model. These fabrics are used as material in socks, especially in diabetic and athletic socks. Since the compression properties of socks affect the plantar pressure, it

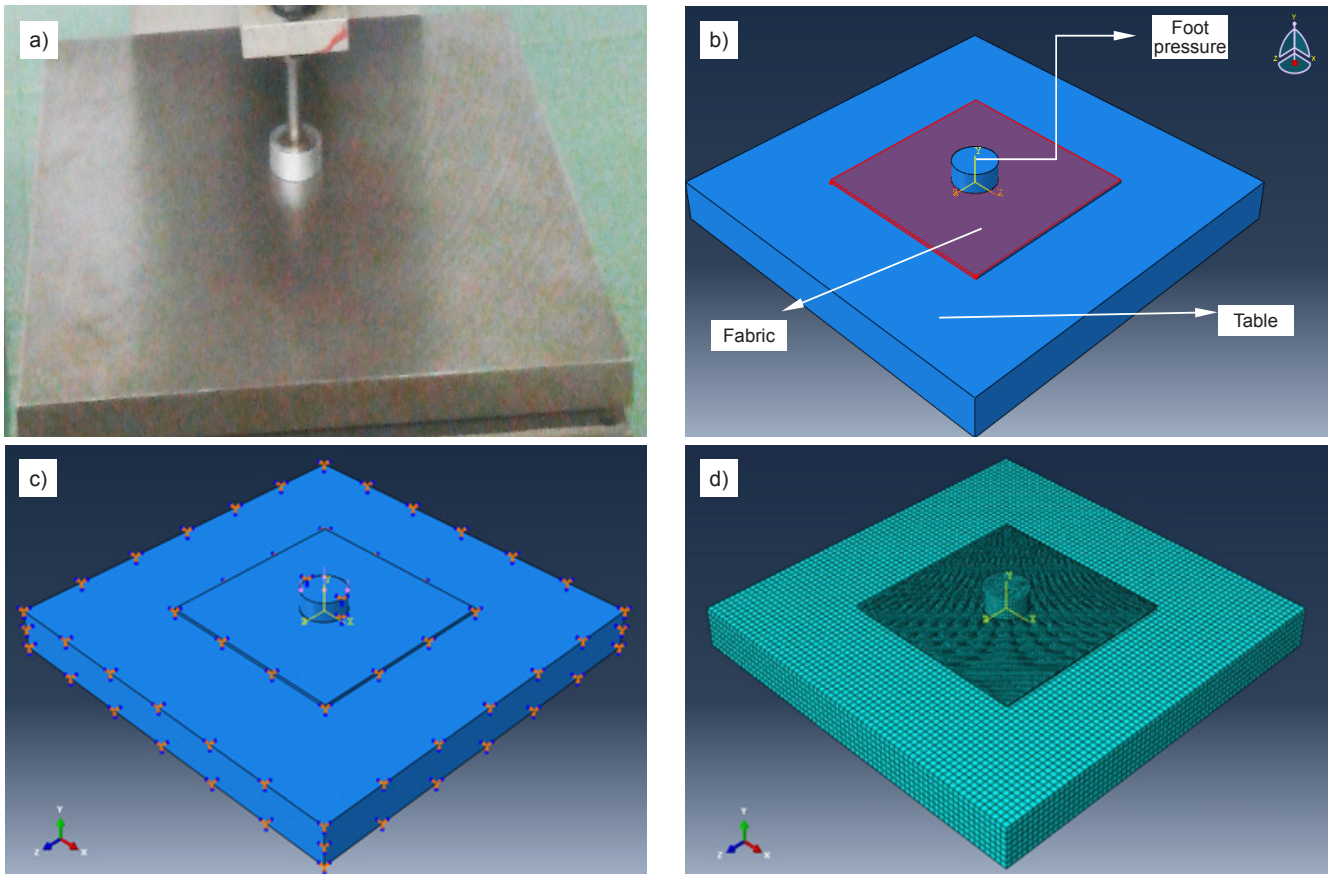


Figure 1. a) Shirley digital thickness tester, b) Simulation of Shirley digital thickness tester in ABAQUS, c) Boundary conditions, d) FE meshes.

is important to predict changes in these properties which occurs due to an applied maximum pressure level similar to that created in diabetic socks during standing and, to some extent, walking. Therefore the objective of this study was to develop a computational modelling approach for FEM analysis of weft-knitted fabric under compression deformation. Thus a 3D finite element model based on the hyperfoam material model was performed in order to predict the compression behaviour of single jersey weft-knitted fabrics and compare the compression parameters with those of experimental results.

Methods

Finite element models

A three-dimensional (3D) finite element model for a fabric compression system was presented. The geometry of the model was simulated using a Shirley digital thickness tester (**Figure 1.a**). The tester consists of a table, foot pressure and dead weights. The fabric was placed between the two platens, where the lower one is a plate and the upper is foot pressure, as shown in **Figure 1.b**. The table was completely constrained and the foot pressure can be moved only in the Y direction.

Compression was applied at a constant pressure rate on the foot pressure (**Figure 1.c**). Due to geometrical nonlinearities, the model is analysed according to large strain theory, i.e. the nonlinear geometry option was used. Multiple contacts were defined between fabric surfaces with the platens using surface-surface contact. The Lagrange multiplier and Penalty methods are most often used to formulate the contact constraints. The Lagrange multiplier method is usually used for the non-penetration contact interface and the Penalty method for the contact condition, where penetration is allowed. It can be noted that the penalty parameter has a physical interpretation, representing the stiffness of a fictitious spring which joins the points of an active pair. Because this constraint is unilateral this spring can only be compressed. In order to fulfil the constraint condition, this spring would need to be of infinite stiffness. This interpretation leaves some space for an interesting approach where the stiffness value might be adopted in a way to represent real elastic properties of the surfaces of the contacting bodies. The Lagrange multiplier represents a force normal to the contacting surfaces. This value is unknown and does change

during the process, hence it is clearly justified that it must be considered as an extra unknown in the problem.[12]. Thus the Lagrange multiplier method is used in this study. The friction between the two platens and the fabric is neglected.

Eight-node linear brick elements were used to mesh the table and foot pressure (**Figure 1.d**).

A mesh with an approximate element length of 0.7 mm was found to provide sufficient precision in spatial displacements. Five elements were inserted into the thickness of the fabric. The change in spatial displacement was not more than 2% with a further increase in mesh density (**Figure 1.d**).

Two compression platens, the table and foot pressure, were assumed to be rigid with steel properties ($E = 200$ GPa and Poisson's ratio = 0.3).

Experimental

Fabric samples

Nine different knitted fabrics previously produced by author [7] were used in this study. A commercial high-bulk acrylic yarn (61.3% shrinkable fibre of 3.33 dtex,

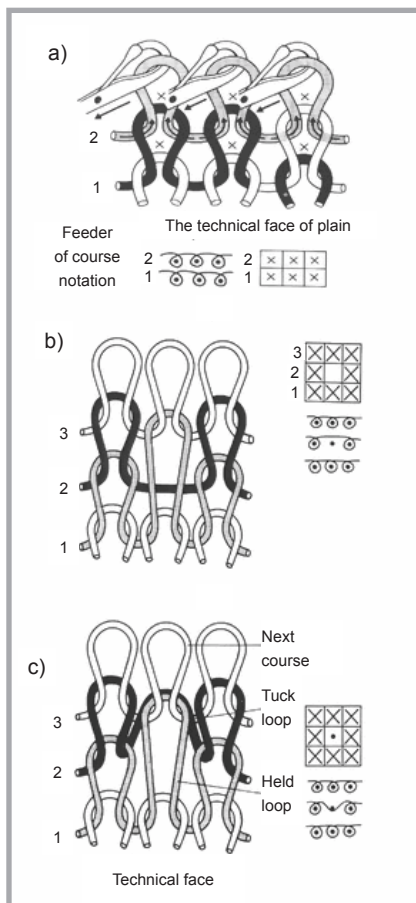


Figure 2. Single jersey weft-knitted fabrics with a) plain, b) knit-miss, and c) knit-tuck structures [7].

32.6% non-shrinkable fibre of 3.33 dtex and 6.1% non-shrinkable of 5.55 dtex (linear density) with an average yarn count of 30/2 N_m was utilized to knit the fabrics. Knitted fabric samples were produced on a single jersey flat knitting machine (A.R.S.D, R88-96 Mode, China). The machine gauge was 8 (needle/inch), the fabric width 50 cm (163 needles), and the cam setting numbers for different loop lengths were adjusted to 15(1), 16(2) and 17(3). Single jersey weft knitted fabrics were produced with three different structures including plain (P), knit-miss (M) and knit-tuck (T), and three

different loop lengths (high, medium and low). **Figure 2** shows these three fabric structures. A summary of the fabric-construction parameters for three fabric structures at three different loop lengths is presented in **Table 1**.

Compression testing

In order to investigate fabric compression properties, we used a Shirley digital thickness tester [7, 13]. By using this thickness tester, it was possible to measure fabric thickness at different pressures including 20, 50, 100, 200, 500, 1000, 1500 and 2000 g/cm^2 (corresponding to 2.04, 5.10, 10.19, 20.39, 50.97, 101.94, 152.90, and 203.87 kPa pressure respectively). The first compression reading was taken at 30 seconds under a pressure of 20 g/cm^2 . Thus the thickness at 20 g/cm^2 pressure was recorded as the initial thickness (T_0). Subsequently the pressure was increased from 20 in steps to 50, 100, 200, 500, 1000, 1500 and 2000 g/cm^2 and the corresponding compression readings were recorded using the same procedure. The fabric thickness under a maximum pressure of 2000 g/cm^2 (P_m) was registered as the minimum thickness (T_m).

Physical model

In clothing, especially in the sole of socks, good compression hardness in fabric means that cushions don't „bottom out”, „feel through” or compress to the point where they no longer hold up the weight of a person. It also means that the cushion is capable of distributing the weight of the person for maximum comfort.

A typical loading curve of weft knitted fabric is shown in **Figure 3**. It may be considered that the compression curve of the weft-knitted structure consists of three zones. At low pressure, the protruding hair fibres from the outer surface of the fabric are compressed and the compression characteristic in this first region is presumed to be elastic. Increasing

the pressure overcomes the internal fibre and yarn friction, and fibre slippage takes place. Thus in this second region, the fabric thickness decreases nonlinearly with increasing pressure. Further increasing the pressure compresses the fibres laterally, and in this third region, a highly packed fibre assembly can be considered. In this simulation, the stress-strain behaviour of weft knitted fabric was represented by the hyperfoam strain energy function and the material properties were obtained by fitting the hyperfoam model to the nonlinear stress-strain data obtained during uniaxial compression tests of samples with uniform geometry. The behaviour of this kind of fabric is similar to latex foam [14].

Governing equations

It is necessary to note that several preliminary works were carried out in order to ascertain what type of material can be assumed for knitted fabric.

In the first step, knitted fabric was modelled as a continuous solid body with linear elastic material, but the results were not acceptable since this material is valid for small elastic strains (normally less than 5%) [15], as compared with our samples, which exhibit a compressive strain around 70%. In the second step, it was decided to use a hyperelastic model in order to define the knitted fabric material property. The hyperelastic model is valid for large elastic strains, but this nonlinear elasticity model also provides the general strain energy potential to describe the material behaviour for nearly incompressible elastomers [15], and therefore it cannot be considered for highly compressible knitted fabric.

Indeed fabrics consist of fibre and air. In this research work, we assumed that the fabrics are typical porous elastic material. Porous materials are commonly found in nature and as industrial materials such as wood, carbon, foams and fabric. A porous material is a material containing pores (voids). The skeletal portion of the material is often called the „matrix” or „frame”. The pores are typically filled with a fluid (liquid or gas) [16]. However, porous elastic materials are valid for small elastic strain (normally less than 5%) [15]. Hyperfoam materials can deform elastically under large strains, up to 90% strain in compression. For these reasons, we assumed that fabric behaviour is similar to hyperfoam materials and the fabric was modeled with hyperfoam material, which is highly compressible.

Table 1. Construction parameters of fabrics tested [7].

Fabric ID	Course per centimetre, C.P.C	Wale per centimetre, W.P.C	Stitch density, cm^{-2}	Mass per unit, g/m^2	Weave
P1	5.84	4.64	27.10	180.5	Plain
P2	4.70	4.35	20.45	152.5	
P3	4.15	3.98	16.50	142.0	
M1	7.35	4.40	32.34	195.0	Knit-miss
M2	6.40	4.15	26.56	181.5	
M3	5.40	4.00	21.60	163	
T1	7.75	3.30	25.58	184.0	Knit-tuck
T2	7.10	2.95	20.95	178.0	
T3	6.10	2.80	17.08	149.5	

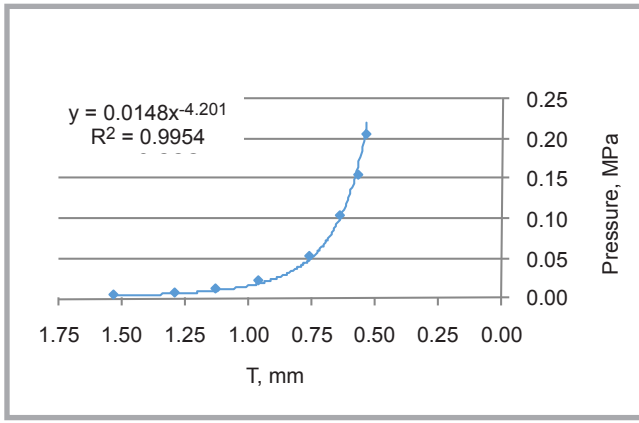


Figure 3. Pressure-thickness curve of a typical fabric (Fabric ID: P1).

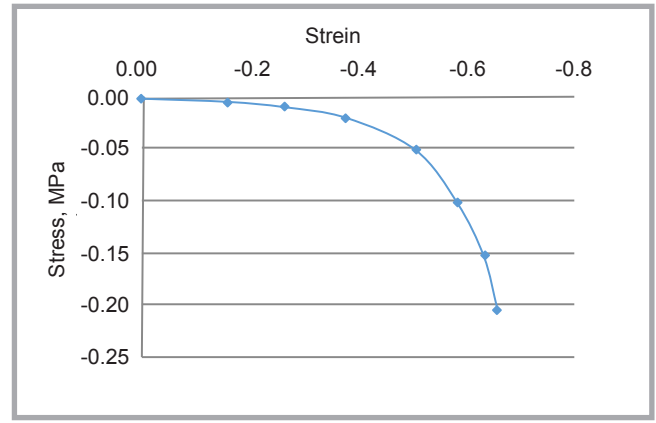


Figure 4. Pressure-thickness curve of a typical fabric (Fabric ID: P1).

In order to use porous materials effectively, their mechanical properties must be understood in relation to their microstructures. Detailed information required consists of the density, porosity, surface area and pore size distribution [16].

Porous materials react differently to compressive stress than fully consolidated materials. The added complication introduced by porosity is that changes in a material's bulk density are due to both the closing of the pore space (compaction) and compression of the solid component, referred to here as the matrix. The amount of resistance to volume change and the amount of irreversible work done during these two processes is very different; it is far easier to compact a porous material sample than to compress a nonporous sample of the same material. In this regard a porous-compaction model is basically a way of describing the compression of the pore space as a function of compressive stress.

To adapt the fabrics based on a porous material model, the density of the material is actually the fabric density and the density of the solid component is the yarn density [17].

$$\varepsilon = 1 - \frac{\rho_{fabric}}{\rho_{yarn}} \quad (1)$$

where, ε is the porosity expressed as a coefficient, and the fabric density (ρ_{fabric}) depends on the fabric weight and thickness, as shown in **Equation 2**:

$$\rho_F = m_F/d_F \quad (2)$$

where, ρ_F - fabric density in kg/m^3 , m_F - fabric weight in g/m^2 , d_F - fabric thickness in mm.

The yarn density (ρ_{yarn}) is equal to the fibre density (ρ_{fibre}) times the yarn packing fraction (Φ). In this work, the fibre densi-

ty and yarn packing fraction are assumed to be 1.46 g/cm^3 and 60% , respectively.

In a highly compressible elastomeric foam material model, the elastic behaviour of the foams is based on the strain energy function **Equation 3** [15] where, $\hat{\lambda}_{1-3}$ are the principal stretches, and J^{el} is the elastic volume ratio with $\hat{\lambda}_1 \hat{\lambda}_2 \hat{\lambda}_3 = J^{el}$. N , μ_i , α_i and β_i are material parameters and

$$\beta_i = \frac{\nu_i}{1 - 2\nu_i} \quad (4)$$

where, ν is Poisson's ratio.

In FEM analysis, the fabric was compressed up to 50% of its initial thickness in eight steps similar to that used in the experimental investigation. In each step, the displacement and force were measured simultaneously and normalised by the sample thickness and area, respectively, to calculate the nominal strain and

stress, respectively. Stress-strain data of different fabric materials (**Figure 4**) were used to extract (root-mean-square of fit error < 2% maximum stress) material parameters of the hyperfoam material model (**Equation 3**) in ABAQUS (**Table 2**) [15].

In the model, the initial pressure was defined at the 2.04 kPa value. Then seven steps corresponding to seven pressure values of 5.1, 10.19, 20.39, 50.97, 101.94, 152.90, and 203.87 kPa were defined according to the experimental method. By using this method, it is possible to measure the fabric thickness at different pressure values.

Parameters investigated

The compression parameters include the work of compression WC (fabric compression energy under 196 kPa pressure), the linearity of compression LC

$$U = \sum_{i=1}^N \frac{2\mu_i}{\alpha_i^2} \left[\hat{\lambda}_1^{\alpha_i} + \hat{\lambda}_2^{\alpha_i} + \hat{\lambda}_3^{\alpha_i} - 3 + \frac{1}{\beta_i} \left((J^{el})^{-\alpha_i \beta_i} - 1 \right) \right] \quad (3)$$

$$WC = \int_{T_0}^{T_m} P dt = \int_{T_0}^{T_m} a T^b dt = \frac{a}{b+1} (T_m^{b+1} - T_0^{b+1}) \quad (6)$$

Equations 3 and 6.

Table 2. Properties and coefficients of the hyperfoam material model used for simulated fabric in FEM.

Fabric ID	Initial thickness (T_0), mm	Density, kg/m^3	Initial void ratio	μ , MPa	α	β
P1	1.53	117.97	0.816	9.59	5.61	2.00
P2	1.48	103.04	0.839	9.41	5.39	1.80
P3	1.49	95.30	0.851	7.56	5.22	0.75
M1	1.90	102.63	0.840	5.71	5.47	0.97
M2	1.87	97.06	0.848	4.71	4.80	2.48
M3	1.72	94.77	0.852	4.95	4.89	2.62
T1	1.91	96.34	0.849	8.19	4.85	0.75
T2	1.96	90.82	0.858	5.87	4.31	2.62
T3	2.01	74.38	0.884	3.48	4.46	1.75

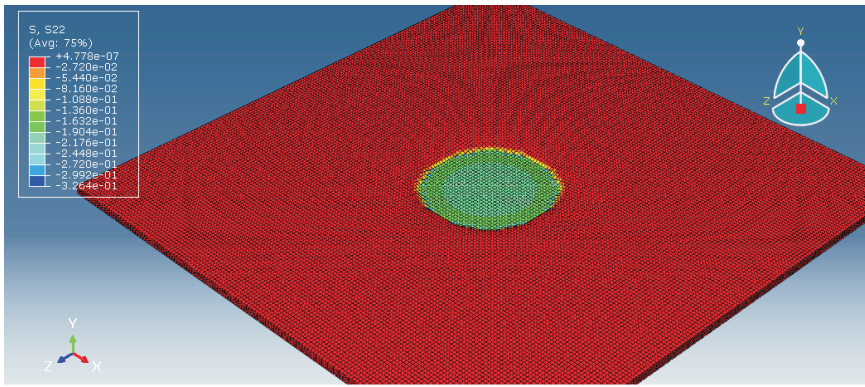


Figure 5. Distribution of pressure on the fabric (Fabric ID: P1).

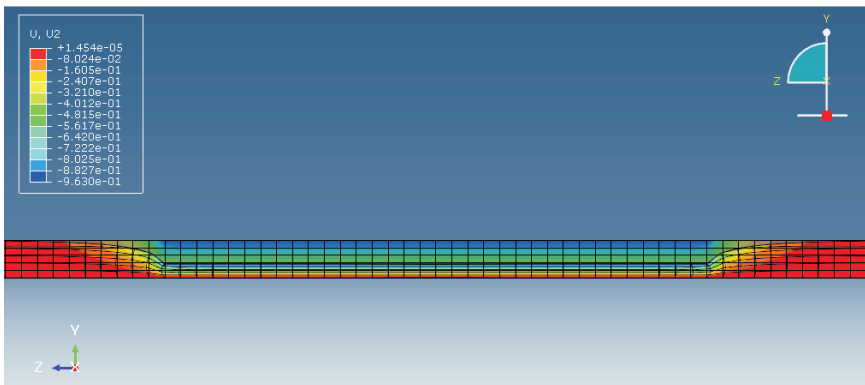


Figure 6. Fabric thickness on deformed and undeformed fabric (Fabric ID: P1).

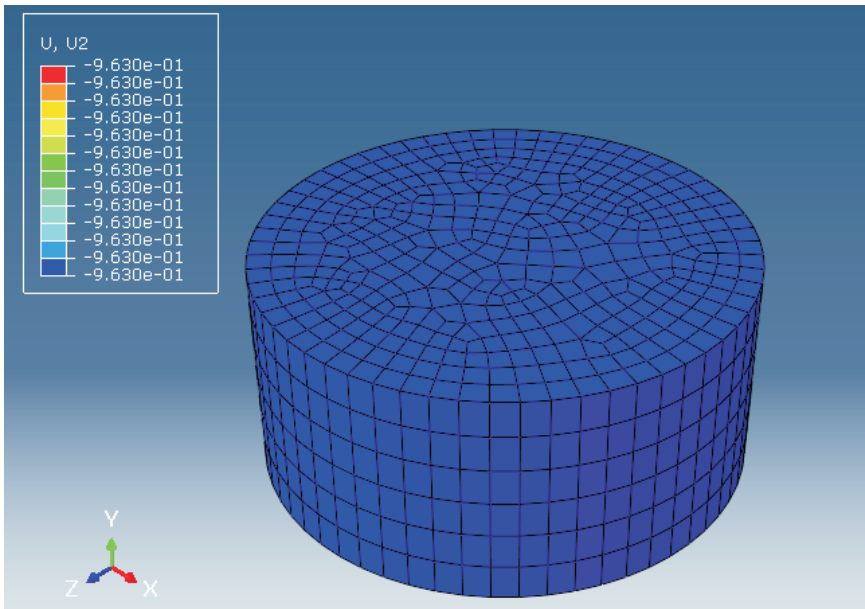


Figure 7. Contour of + foot pressure displacement according to fabric thickness changes (Fabric ID: P1).

(Linearity of compression/thickness curve) and relative compressibility EMC (percentage reduction in fabric thickness resulting from an increase in the lateral pressure from 20 to 2000 gf/cm²), and the fabric compression deformation or fabric surface thickness ΔT are calculated.

A typical pressure-thickness curve of fabric obtained by the experimental method is shown in **Figure 3**. Taking the power trend line fitted for each fabric based on $P = a T^b$ (P is pressure, T thickness, and a & b are constants), then the work of compression is equal to **Equation 6** (see page 85).

In the FEM analysis approach, the WC parameter is calculated using the history output. Thus other compression parameters in FEM analysis are calculated accordingly.

$$LC = \frac{WC}{\frac{P_m}{2}(T_0 - T_m)} \quad (7)$$

$$EMC = 1 - \frac{T_m}{T_0} \quad (8)$$

$$\Delta T = T_0 - T_m \quad (9)$$

The compressional work per unit area, WC in cN cm/cm², varies depending on the type of fabric. A more compressible material gives larger values.

The second distinctive parameter for compression is the linearity of compression (LC). If the thickness of the fabric decreases linearly with increasing pressure, the LC value would be 1. However, all fabrics compress non-linearly, and have an LC value ranging between 0.24 to 0.35. The harder fabrics have a lower value of LC, which would result in a steeper rising compression. The dimensionless EMC parameter expresses the compressibility of a fabric. The smaller the EMC value, the harder the fabric in compression.

Results and discussion

Figure 5 illustrates the distribution of stress on the fabric. It is seen that stress concentration appears in the intersection regions between the table and foot pressure. Negative values of stress show the pressure on it. The maximum pressure is 0.203 MPa, which is an acceptable pressure according to the maximum pressure of compression defined in step 7. **Figure 6** shows the initial thickness (T_0) and final thickness (T_m) under a compressive load. **Figure 7** shows the changes in foot pressure displacement along the Y direction equal to fabric thickness changes.

The average values of fabric compression properties for different fabric structures obtained by experimental and FE modelling are shown and compared in **Table 3**. **Figure 8** shows the displacement and stress of foot pressure in seven steps of loading. According to these results, the compression curve of weft-knitted fabric was plotted. A typical curve of pressure against fabric thickness changes (experimental and finite element results) is shown in **Figure 9**.

FEM results show that while the porous material structures considered here

change from plain to knit-miss and knit-miss to knit-tuck, the density is increased and the initial void ratio (ϵ) is decreased (Table 2); and consequently the compressibility of the porous material is increased. As a consequence, the surface thickness (ΔT), fabric compression energy (WC) and compressibility of the fabric (EMC) significantly increase (Table 3). On the other hand, the coefficients of the hyperfoam material model decrease with an increase in the loop length of weft-knitted fabrics, which in turn leads to a decrease in fabric compression energy (WC).

The FE modeling results obtained indicate fairly good agreement with experimental results (Table 3 and Figure 10). The average error of fabric thickness changes predicted is 5 percent. The slight difference between the results may be due to the short fibres with low density over the fabric surface, which was ignored in the FE model. In the model, it was assumed that the fabric is a homogeneous hyperfoam. However, the real fabric is more compressible than in the model, and hence the experimental compression energy (WC) and fabric compressibility (EMC) values are smaller than the FEM results. The difference between the linearity of compression (LC) results may be due to ignoring the friction effect in the model. In general, as shown in Figure 10, the variation trend of compression parameters against knitted fabric types for two experimental and FEM analysis results is almost similar.

Conclusions

Unlike experimental measurements, finite element analysis has the benefit of quantifying the overall deformation, stress, strain, and displacement distribution of a structure to be analysed. In

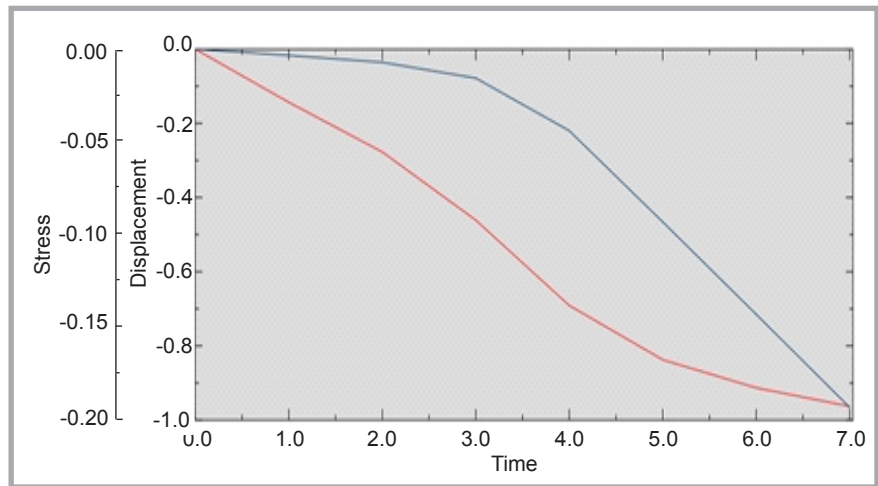


Figure 8. Spatial displacement and stress at a node on the fabric (Fabric ID: P1); — - U: U2 P1: Fabric-1 N: 68782, — - S: S22(Avg: 75%) P1: Fabric-1 N: 68782.

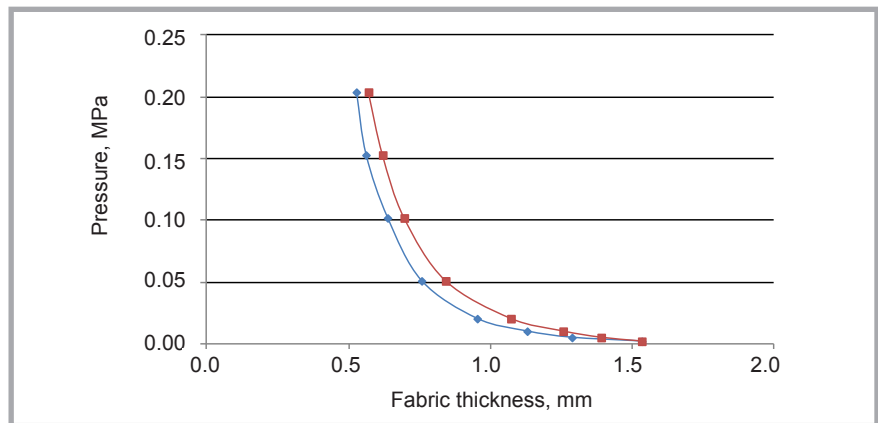


Figure 9. Typical curve of pressure against fabric thickness changes (Fabric ID: P1), (Experimental and FEM analysis); ◆ - experimental, ■ - finite element result.

this study, a FE compression model was developed for knitted fabric based on porous material behaviour. Nonlinear geometric and linear material behaviours are used in the model. The strains predicted by the model were in good agreement with those measured during compressive loading. In general, this 3D model confirms the compression

properties of single jersey weft knitted fabrics to be used as the planar of socks.

One of the major advantages of the model proposed over other approaches is that all kinds of textile fibre assemblies under compressive loading can be modelled. The modelling approach proposed in this

Table 3. Fabric compression parameter results.

Fabric ID	ΔT , mm		Error, %	WC cN.cm/cm ²		Error, %	LC, %		Error, %	EMC, %		Error, %
	Experimental	FE model		Experimental	FE model		Experimental	FE model		Experimental	FE model	
P1	1.01	0.96	4.6	37.37	42.99	-15.0	37.00	44.64	-20.6	65.66	62.85	4.3
P2	0.98	0.96	2.4	36.59	42.37	-15.7	37.34	44.32	-18.7	66.39	64.59	2.7
P3	1.03	0.99	4.1	32.76	41.15	-24.5	33.63	36.62	12.2	68.77	66.31	3.6
M1	1.34	1.25	6.5	41.07	51.81	-26.2	30.65	38.67	-26.2	70.53	65.95	6.5
M2	1.39	1.32	5.3	39.38	50.71	-28.8	28.33	38.53	-36.0	74.33	70.37	5.3
M3	1.27	1.20	5.7	37.30	46.80	-25.5	29.37	39.06	-33.0	73.46	69.65	5.2
T1	1.32	1.26	4.8	43.87	55.33	-26.1	33.24	42.69	-28.4	69.40	65.76	5.3
T2	1.45	1.34	7.8	41.14	51.17	-24.3	28.37	38.30	-35.0	73.98	68.16	7.9
T3	1.55	1.50	3.4	38.06	49.49	-30.0	24.55	33.04	-34.6	77.23	74.53	3.5

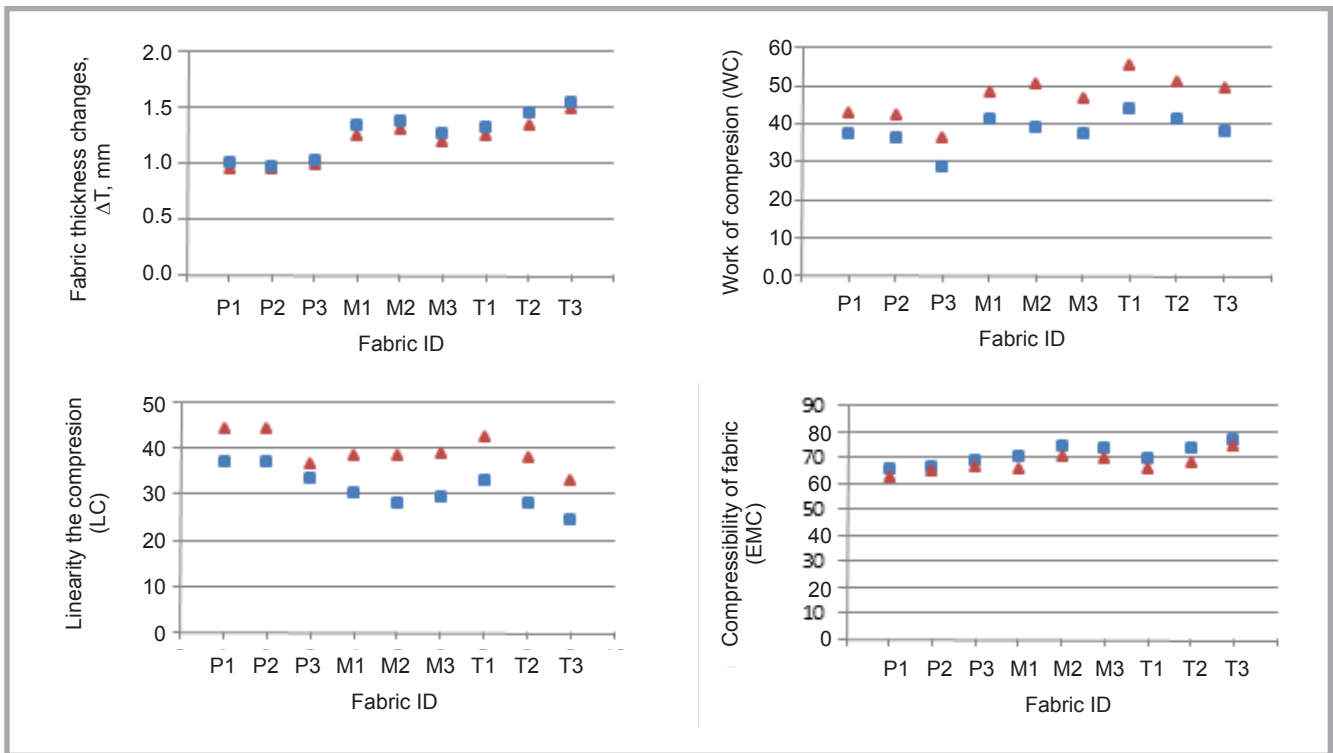


Figure 10. Comparison between experimental and finite element results; ■ - experimental, ▲ - finite element result.

research study provides a new window into the simulation and modeling of knitted fabric structures under static compression loading. But further research is needed to model these structures at a meso scale level in order to get a deeper understanding of their behaviour under compression loading.

It is expected that FE methods will play an important role in the future development of socks designed, using a material that has the best compression properties.

References

- Gunasekaran G, et al. Evaluation of a new single parameter for characterising the compressional properties of weft-knitted fabrics. *Indian Journal of Fiber & Textile Reserch*, 2011; 36: 242-247.
- van Wyk CM. Note on the Compressibility of Wool. *J. Text. Inst* 1946; 37: 285-292.
- de Jong S, Snaith JW and Michie NA. A Mechanical Model for the Lateral Compression of Woven Fabrics. *Text. Res. J* 1986; 56: 759-767.
- Beil NB and Roberts WW. Modeling and Computer Simulation of the Compressional Behavior of Fiber Assemblies: Part I: Comparison to van Wyk's Theory. *Text. Res. J.* 2002; 72: 341.
- Gurumurthy BR, Prediction of Fabric Compressive Properties using Artificial Neural Networks. *Autex Research Journal* 2007; 7(1): 19.
- Murthyguru, Novel approach to Study Compression Properties in Textile. *Autex Research Journal* 2005; 5(4): 176.
- Bakhtiari M, Shaikhzadeh Najar S and Etrati SM. Compression Properties of Weft Knitted Fabrics Consisting of Shrinkable and Non-Shrinkable Acrylic Fibers. *Fibers and Polymers* 2006; 7(3): 295-304.
- Xu-hong M. and Ming-qiao G. The Compression Behaviour of Warp Knitted Spacer Fabric. *Fibres and Textiles in Eastern Europe* 2008; 16(1): 90.
- Lin H, et al. Finite element modelling of fabric compression. *Modelling and Simulation in Materials Science and Engineering* 2008; 16: 1.
- Vassiliadis S, et al. Numerical Modelling of the Compressional Behaviour of Warp-knitted Spacer Fabrics. *Fibres and Textiles in Eastern Europe* 2009; 17(5): 56.
- Sheikhzadeh M, et al. A modeling study on the lateral compressive behavior of spacer fabrics. *J. Text. Inst.* 2010; 101(9): 795-800.
- Wriggers P. *Computational Contact Mechanics*. 3rd ed. 2002.
- Shirley Development Ltd. 2005.
- Alzoubi MF, Al-Hallaj S and Abu-Ayyad M. Modeling of Compression Curves of Flexible Polyurethane Foam with Variable Density. *Chemical Formulations and Strain Rates* 2014; 6(1): 82-97.
- ABAQUS theory and user's manual, version 6.8. ABAQUS theory and user's manual, version 6.8, 2008.
- Lu G, Lu GQ and Xiao ZM. Mechanical Properties of Porous Materials. *Journal of Porous Materials* 1999; 6: 359-368.
- Dubrovski P and Brezočnik M. *The Usage of Genetic Methods for Prediction of Fabric Porosity*, 2012.

Received 18.02.2014 Reviewed 06.08.2015

Fibres and Textiles in Eastern Europe